Supporting Information

In Situ Formation of N-Heterocyclic Carbene-Bound Single-Molecule Junctions

Evan A. Doud,[†,⊥] Michael S. Inkpen,[‡,⊥] Giacomo Lovat,[‡] Enrique Montes,[§] Daniel W. Paley,[∥] Michael L. Steigerwald,[†] Héctor Vázquez,*[,§] Latha Venkataraman,*[,†,‡] and Xavier Roy*[,†]

[†]Department of Chemistry, Columbia University, New York, NY 10027, USA.

[‡]Department of Applied Physics and Applied Mathematics, Columbia University, New York, NY 10027, USA.

[§]Institute of Physics, Academy of Sciences of the Czech Republic, Cukrovarnická 10, Prague, CZ 16200, Czech Republic.

[∥]Columbia Nano Initiative, Columbia University, New York, New York 10027, United States

[⊥] Contributed equally to this work.

* vazquez@fzu.cz, lv2117@columbia.edu, xr2114@columbia.edu

Table of Contents

1. Synthetic Details

General Information. 2-Iodopropane and sodium metal were purchased from Acros Organics. Ammonium chloride was purchased from Alfa Aesar. DMSO-d_6, benzene-d_6, and $CDCl_3$ were purchased from Cambridge Isotope. Dichloromethane (DCM), diethyl ether, dioxane, ethyl acetate, hexanes, isopropanol, sodium chloride, and tetrahydrofuran (THF) were purchased from Fisher Scientific. 5-Chloro-2-nitroaniline was purchased from Matrix Scientific. Silica gel was purchased from Silicycle. All other reagents and solvents were purchased from Sigma-Aldrich. Dry and deoxygenated solvents were prepared by elution through a dual-column solvent system (MBraun SPS). All reactions and sample preparations were carried out under inert atmosphere using standard Schlenk techniques or in a nitrogen-filled glovebox unless otherwise noted.

An overall synthetic scheme is given in Figure S1.

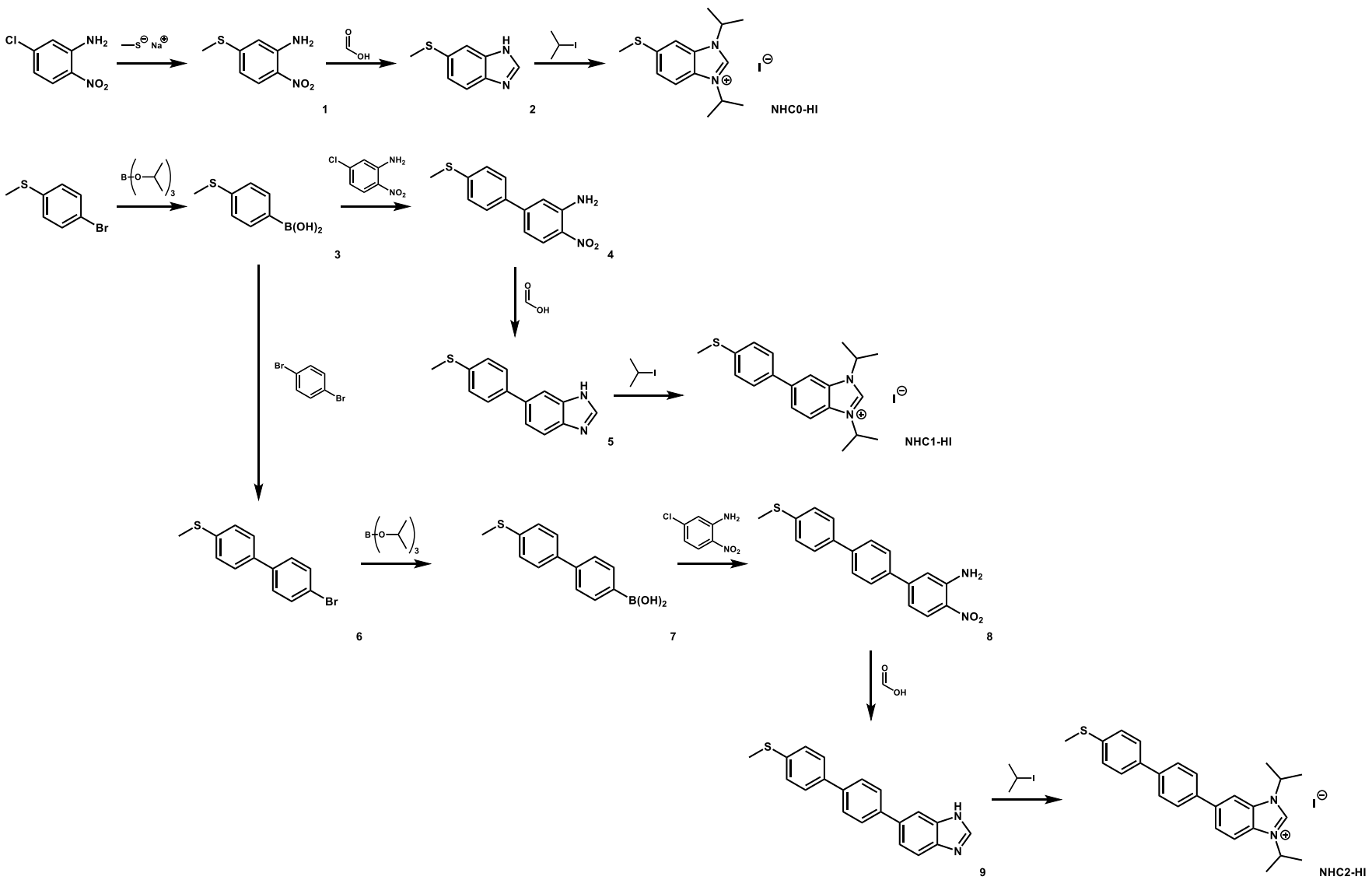

Figure S1: Synthetic scheme for the synthesis of NHC precursors. Full synthetic details are given below.

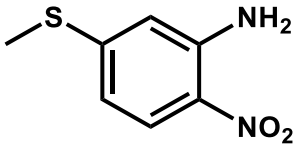

1

1. An oven-dried 250 mL round bottom flask equipped with a Teflon coated stir bar was charged with sodium methanethiolate (3.04 g, 43.4 mmol) (prepared according to a literature procedure[1]). Dry and deoxygenated N,N-dimethylformamide (DMF) (50 mL) was added and the suspension was vigorously stirred for 30 minutes. A solution of 5-chloro-2-nitroaniline (5.00 g, 28.9 mmol) in 50 mL of dry and deoxygenated DMF was added via oven-dried cannula to the sodium methanethiolate suspension. The reaction mixture turned a light red color and was then heated to 65°C for 20 hours or until TLC indicated complete consumption of the 5-chloro-2-nitroaniline. After 20 h, the deep red reaction mixture was cooled to room temperature and opened to air; 100 mL of water was added, and the reaction mixture was stirred for 1 h. The reaction mixture was then transferred to a separatory funnel and extracted several times with ethyl acetate (5 x 100 mL, a brine solution may be added to facilitate separation of the layers). The combined organic extracts were then washed with water (3 x 250 mL) and brine (2 x 100 mL). The organic extracts were then dried over $MgSO_4$, and the solvent was removed via rotary evaporation. The solid was purified using silica gel flash column chromatography, eluting with 50% ethyl acetate in hexanes to afford **1** as a red-orange solid. (Yield: 4.6 g, 87%)

^{1}H NMR (500 MHz, DMSO-d_6): δ (ppm) 7.86 (d, J = 9.1 Hz, 1H), 7.46 (s, 2H), 6.79 (d, J = 2.1 Hz, 1H), 6.48 (dd, J = 9.1, 2.1 Hz, 1H), 2.48 (s, 3H). ^{13}C{^{1}H} NMR (126 MHz, DMSO-d_6): δ (ppm) 148.80, 146.37, 127.53, 125.60, 113.26, 112.11, 13.83.

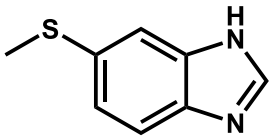

2

2. Synthesized following a modified literature procedure[2]. A 250 mL 2-neck round bottom flask equipped with a Teflon coated stir bar, reflux condenser with gas inlet adapter, and rubber septum, was charged with **1** (2.00 g, 10.8 mmol), Fe powder (6.06 g, 108.5 mmol), and ammonium chloride (5.81 g, 108.5 mmol). The flask was evacuated and refilled with N_2. In a separate 100 mL round bottom flask equipped with a stir bar and rubber septum, 35 mL of formic acid and 50 mL of isopropanol was sparged with N_2 for 15 min. After sparging, the formic acid and isopropanol

solution was added to the flask containing 5-(methylthio)-2-nitroaniline, Fe powder, and ammonium chloride via cannula. The reaction mixture was heated to reflux at 80°C and stirred under N_2 for 3 h. The reaction mixture underwent several color changes finally ending in a light yellow-green with a large amount of gray precipitate. After 3 h, the reaction mixture was cooled to room temperature, opened to air and filtered through a pad of Celite over a medium porosity frit. The filter cake was washed with isopropanol (3 x 20 mL). The combined filtrate was evaporated to dryness via rotary evaporation, leaving a sticky solid. Saturated aqueous $NaHCO_3$ solution was slowly added to the solid residue until a neutral pH was obtained. The reaction mixture was then transferred to a separatory funnel and extracted with chloroform (3 x 50 mL). The combined extracts were dried over $MgSO_4$, filtered, and the solvent was removed via rotary evaporation to yield **2** as a sticky, brown, foamy solid. (Yield: 1.6 g, 90%)

^{1}H NMR (500 MHz, $CDCl_3$): δ (ppm) 8.10 (s, 1H), 7.59 (m, 2H), 7.28 (dd, J = 8.5, 1.7 Hz, 1H), 2.52 (s, 3H). $^{13}C\{^1H\}$ NMR (126 MHz, $CDCl_3$): δ (ppm) 141.35, 138.51, 136.88, 132.54, 123.72, 116.18, 114.35, 17.59.

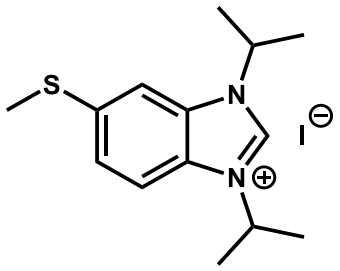

NHC0-HI

NHC0–HI. Synthesized following a modified literature procedure.[2] A 2-neck 100 mL round bottom flask equipped with a Teflon coated stir bar, reflux condenser with a gas inlet adapter, and rubber septum was charged with **2** (0.60 g, 3.6 mmol), K_2CO_3 (1.00 g, 7.2 mmol) and 25 mL of acetonitrile. The reaction mixture was sparged with N_2 while stirring vigorously for 30 min. 2-Iodopropane (2.5 mL, 25 mmol) was then added using a N_2 flushed syringe. The reaction mixture was refluxed at 90°C and stirred for 48 h. The reaction mixture was then cooled to room temperature and all volatiles were removed *in vacuo*. The flask was opened to air, the solid residue was sonicated in 50 mL of DCM for 10 min, and filtered through a pad of Celite over a medium porosity frit. The filter cake was washed with DCM (2 x 20 mL). The DCM filtrate was concentrated by rotary evaporation and ethyl acetate was added to induce precipitation. The suspension was then sonicated for 1 h, the solid was collected by filtration and washed with ethyl

acetate and diethyl ether. The solid was then dried *in vacuo* to yield **NHC0–HI** as an off-white powder. (Yield: 893 mg, 65%)

^{1}H NMR (500 MHz, $CDCl_3$): δ (ppm) 10.82 (s, 1H), 7.70 (d, J = 8.8 Hz, 1H), 7.64–7.41 (m, 2H), 5.18 (overlapping septets, 2H), 2.61 (s, 3H), 1.85 (overlapping d, 12H). ^{13}C{^{1}H} NMR (126 MHz, $CDCl_3$): δ (ppm) 139.81, 139.22, 131.73, 128.45, 126.24, 114.08, 110.19, 52.66, 52.34, 22.35, 22.32, 16.50.

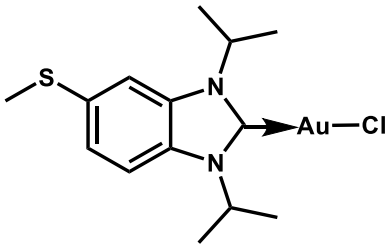

NHC0-AuCl

NHC0–AuCl. Prepared following the general procedure outlined below for the synthesis of **NHC1–AuCl**, using **NHC0–HI** (37 mg, 100 μmol), KO^{t}Bu (12.2 mg, 110 μmol), and $(SMe)_2AuCl$ (32.4 mg, 105 μmol). **NHC0–AuCl** was obtained as a faint yellow powder. (Yield: 46 mg, 95%)

X-ray diffraction quality crystals were grown by slow evaporation of a DCM solution of **NHC0–AuCl**.

^{1}H NMR (500 MHz, $CDCl_3$): δ (ppm) 7.55 (d, J = 8.7 Hz, 1H), 7.51 (d, J = 1.6 Hz, 1H), 7.30 (dd, J = 8.7, 1.7 Hz, 1H), 5.47 (overlapping septets, 7.0 Hz, 2H), 2.56 (s, 6H), 1.72 (overlapping doublets, 12H). ^{13}C{^{1}H} NMR (126 MHz, $CDCl_3$): δ (ppm) 176.37, 134.87, 133.14, 130.53, 123.84, 113.27, 111.53, 54.54, 54.23, 21.73, 21.69, 17.30.

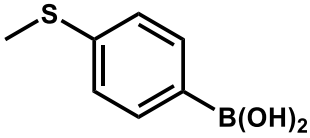

3

3. An oven-dried 3-neck 500 mL round bottom flask equipped with a Teflon coated stir bar, 60 mL addition funnel with a rubber septum, gas inlet adapter, and rubber septum was charged with 50 mL of THF. The flask was cooled to -78 °C in a dry ice/acetone bath, and *n*-BuLi (1.6 M in hexanes, 15 mL, 24.0 mmol) was added to the cooled THF and allowed to stir for 10 minutes. A solution of 4-bromothioanisole (3.00 g, 14.7 mmol) in 50 mL of THF was added to the addition

funnel via a N_2 flushed syringe. The 4-bromothioanisole solution was then added dropwise to the *n*-BuLi solution and the reaction was stirred for 1 h, forming a white slurry. A solution of triisopropyl borate (3.75 g, 20.0 mmol) in 20 mL of THF was then added to the addition funnel using a N_2 flushed syringe. The triisopropyl borate solution was added dropwise; the reaction was warmed to room temperature after the addition finished and was stirred for an additional 3 h. The reaction was then opened to air, 100 mL of water was added dropwise through the addition funnel, and allowed to stir for an additional 30 min. 1M aqueous HCl was slowly added until a pH of 1 was obtained, and the mixture was stirred for 30 min. THF was then removed *in vacuo*. The resulting solid was then filtered and washed with water (3 x 50 mL), hexanes (3 X 50 mL), and dried overnight *in vacuo* to yield **3** as a white fluffy powder. (Yield: 2.05 g, 83%)

^{1}H NMR (500 MHz, DMSO-d_6): δ (ppm) 7.98 (s, 2H), 7.72 (d, J = 8.2 Hz, 2H), 7.21 (d, J = 8.2 Hz, 2H), 2.48 (s, 3H). ^{13}C{^{1}H} NMR (126 MHz, DMSO-d_6): δ (ppm) 140.99, 135.09, 130.28, 124.89, 14.60.

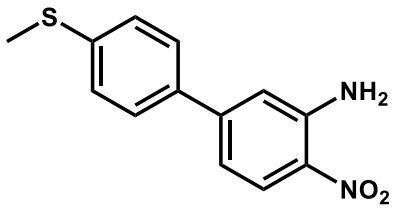

4

4. Synthesized following a modified literature procedure.[3] A 100 mL 2-neck round bottom flask equipped with a Teflon coated stir bar, reflux condenser with a gas inlet adapter, and rubber septum was charged with **3** (1.00 g, 5.9 mmol), 5-chloro-2-nitroaniline (0.80 g, 4.6 mmol) and tri(*o*-tolyl)phosphine (0.44 g, 1.4 mmol). The flask was evacuated and refilled with N_2. In a separate flask, a mixture of 30 mL of dioxane and 10 mL of 2.0 M aqueous K_2CO_3 was sparged with N_2 for 30 min. The mixture was transferred to the 2-neck flask using a cannula and $Pd(PPh_3)_4$ (0.35 g, 0.3 mmol) was added to the flask. The reaction was stirred under reflux for 18 h. The flask was then opened to air and dioxane was removed via rotary evaporation. Ethyl acetate (100 mL) was added to the flask, and the mixture was washed with water (3 x 100 mL) and with brine (2 x 100 mL). The organic phase was dried over $MgSO_4$ and purified by silica gel flash column chromatography, eluting with a 20-50% ethyl acetate in hexanes gradient. **4** was obtained as a yellow crystalline solid. (Yield: 0.99 g, 82%)

^{1}H NMR (500 MHz, DMSO-d_6): δ (ppm) 8.03 (d, J = 9.0 Hz, 1H), 7.61 (d, J = 8.5 Hz, 2H), 7.46 (br, 2H), 7.38 (d, J = 8.5 Hz, 2H), 7.28 (d, J = 2.0 Hz, 1H), 6.93 (dd, J = 9.0, 2.0 Hz, 1H), 2.52 (s, 3H). ^{13}C{^{1}H} NMR (126 MHz, DMSO-d_6): δ (ppm) 146.94, 146.72, 140.18, 134.85, 129.85, 127.65, 126.74, 126.59, 116.24, 114.61, 14.85.

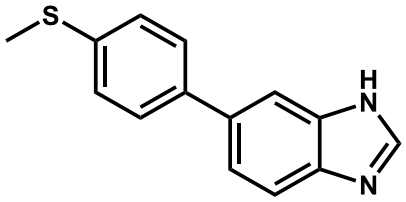

5

5. Synthesized following the same procedure as **2**, starting from **4** (500 mg, 1.9 mmol) with the following modifications. Benzene (100 μL) was added to the reaction to aid solubilizing the amine. After stirring under reflux for 3 h, the mixture was hot filtered. **5** was obtained as a light yellow powder. (Yield: 408 mg, 88%)

^{1}H NMR (500 MHz, DMSO-d_6): δ (ppm) 12.48 (br, 1H), 8.24 (s, 1H), 7.81 (s, 1H), 7.65 (d, J = 8.6 Hz, 3H), 7.48 (dd, J = 8.4, 1.8 Hz, 1H), 7.35 (d, J = 8.4 Hz, 2H), 2.51 (s, 3H). ^{13}C{^{1}H} NMR (126 MHz, DMSO-d_6): δ (ppm) 143.21, 138.22, 136.98, 134.23, 130.25, 127.81, 127.20, 126.98, 121.37, 117.15, 113.92, 15.30.

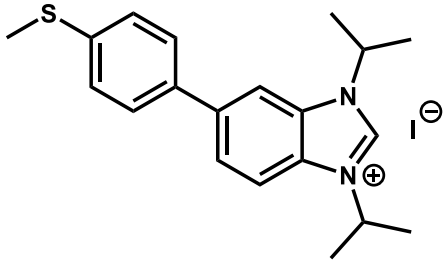

NHC1-HI

NHC1–HI. This compound was synthesized following the same procedure as **NHC0-HI**, starting from **5** (300 mg, 1.2 mmol) with the following modifications. The reaction mixture was heated to reflux and stirred until consumption of the starting benzimidazole material, as determined by NMR (typically 48-96 h). An additional 4 equivalents of 2-iodopropane was added after 48 h if the reaction was not completed. The product was precipitated using a 50:50 mixture of ethyl acetate and diethyl ether. **NHC1–HI** was obtained as an off-white powder. (Yield: 215 mg, 38%)

^{1}H NMR (500 MHz, $CDCl_3$): δ (ppm) 10.91 (s, 1H), 7.89$CDCl_3$, δ ppm): δ –7.79 (m, 3H), 7.54 (d, J = 8.4 Hz, 2H), 7.37 (d, J = 8.4 Hz, 2H), 5.31–5.18 (overlapping septets, 2H), 2.53 (s, 3H), 1.89

(overlapping doublets, 12H). $^{13}C\{^{1}H\}$ NMR (126 MHz, $CDCl_3$): δ (ppm) 140.63, 139.86, 139.81, 135.62, 131.60, 129.91, 127.91, 126.89, 126.62, 114.31, 111.43, 52.70, 52.42, 22.39, 22.34, 15.59.

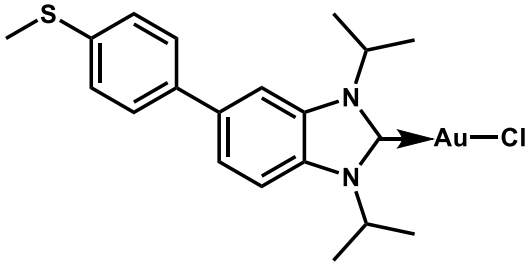

NHC1-AuCl

NHC1–AuCl. Synthesized following a modified literature procedure.[4] **NHC1–HI** (45 mg, 100 μmol) was suspended in 8 mL of THF. KO^{t}Bu (12 mg, 110 μmol) was added to the suspension and the reaction was stirred for 1 h. The mixture was then filtered through Celite and $(SMe)_2AuCl$ (31 mg, 105 μmol) was added to the filtrate. The reaction was stirred for 3 h, protected from light. Activated carbon (~100 mg) was added to the reaction, which was stirred for 1 h and then filtered through Celite. The solvent was then removed *in vacuo*. The solid residue was redissolved in DCM, filtered, and the solvent removed *in vacuo* to yield the pure complex **NHC1–AuCl** as a light yellow powder. (Yield: 48 mg, 86%)

X-ray diffraction quality single crystals were obtained by slow diffusion of hexanes into a DCM solution of the complex.

^{1}H NMR (500 MHz, $CDCl_3$): δ (ppm) 7.76 (d, J = 1.5 Hz, 1H), 7.71 (d, J = 8.6 Hz, 1H), 7.58 (dd, J = 8.6, 1.6 Hz, 1H), 7.54 (d, J = 8.4 Hz, 2H), 7.40 (d, J = 8.4 Hz, 2H), 5.56 (overlapping septets, 2H), 2.57 (s, 3H), 1.79 (overlapping doublets, 12H). $^{13}C\{^{1}H\}$ NMR (126 MHz, $CDCl_3$): δ (ppm) 176.74, 138.74, 137.34, 136.95, 133.15, 131.60, 127.81, 127.00, 123.35, 113.28, 111.07, 54.57, 54.31, 21.80, 21.72, 15.77.

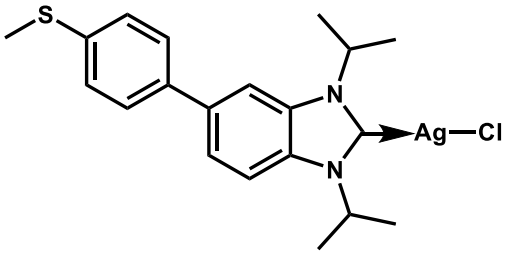

NHC1-AgCl

NHC1–AgCl. Prepared following the general procedure outlined above for the synthesis of **NHC1–AuCl**, using **NHC1–HI** (45 mg, 100 μmol) and (SMe_2)AgCl (20 mg, 105 μmol, see synthesis below). **NHC1–AgCl** was obtained as a light off-white powder. (Yield: 40 mg, 85%)

X-ray diffraction quality crystals were grown by slow evaporation of a DCM solution of **NHC1–AgCl**.

^{1}H NMR (400 MHz, $CDCl_3$): δ (ppm) 7.71 (d, *J* = 1.5 Hz, 1H), 7.66 (d, *J* = 8.7 Hz, 1H), 7.57 (dd, *J* = 6.6, 1.7 Hz, 1H), 7.52 (d, *J* = 8.4 Hz, 2H), 7.37 (d, *J* = 8.5 Hz, 2H), 5.15–5.03 (overlapping septets, 2H), 2.54 (s, 3H), 1.75 (overlapping doublets, 12H). ^{13}C{^{1}H} NMR (101 MHz, $CDCl_3$): δ (ppm) 176.49, 138.66, 137.23, 137.04, 133.90, 132.22, 127.84, 127.81, 127.01, 123.28, 112.93, 110.74, 54.44, 53.98, 22.62, 22.49, 15.79.

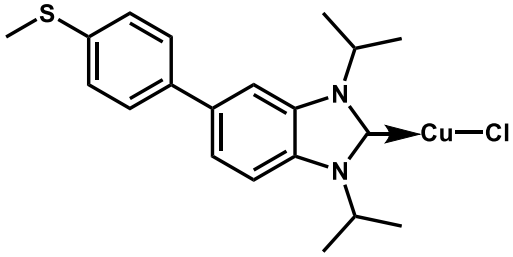

NHC1-CuCl

NHC1–CuCl. Prepared following the general procedure outlined above for the synthesis of **NHC1–AuCl**, using **NHC1–HI** (45 mg, 100 μmol) and (SMe_2)CuCl (16 mg, 105 μmol, see synthesis below). **NHC1–CuCl** was obtained as a white powder. (Yield: 36 mg, 85%)

X-ray diffraction quality crystals were grown by slow diffusion of hexanes into a THF solution of **NHC1–CuCl**.

^{1}H NMR (400 MHz, $CDCl_3$): δ (ppm) 7.66 (d, *J* = 1.4 Hz, 1H), 7.60 (d, *J* = 8.6 Hz, 1H), 7.56 (d, *J* = 1.5 Hz, 1H), 7.52 (d, *J* = 8.5 Hz, 2H), 7.37 (d, *J* = 8.4 Hz, 2H), 5.08 (overlapping septets, 2H), 2.54 (s, 3H), 1.79 (overlapping doublets, 12H). ^{13}C{^{1}H} NMR (101 MHz, $CDCl_3$): δ (ppm) 180.95, 138.52, 137.18, 137.11, 133.82, 132.24, 127.81, 127.03, 123.12, 112.33, 110.11, 52.95, 52.45, 23.17, 23.02, 15.81.

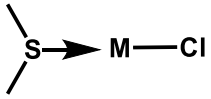

(SMe_2)MCl. Both (SMe_2)CuCl and (SMe_2)AgCl were synthesized using the same procedure. CuCl (99 mg, 1.0 mmol) or AgCl (143 mg, 1.0 mmol) was stirred in 10 mL of dimethylsulfide for 12 hours (with protection from light in the case of AgCl). The reaction mixture was filtered and hexanes was added to precipitate the product. The solid was collected by filtration, washed with diethyl ether and dried *in vacuo*. (SMe_2)CuCl (yield: 147 mg, 91%) was obtained as a colorless crystalline solid, and (SMe_2)AgCl (yield: 180 mg, 88%) was obtained as a white powder.

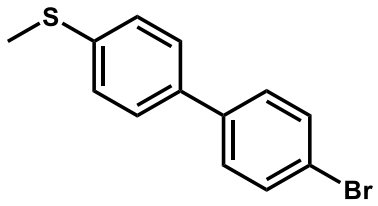

6

6. A 250 mL 2-neck round bottom flask equipped with a Teflon coated stir bar, reflux condenser with a gas inlet adapter, and rubber septum was charged with **3** (2.00 g, 11.9 mmol), 1,4-dibromobenzene (5.62 g, 24.0 mmol), and $PdCl_2(PPh_3)_2$ (0.25 g, 0.35 mmol). The flask was evacuated and refilled with N_2. In a separate flask, a mixture of 50 mL of dioxane and 25 mL of 2.0 M aqueous K_2CO_3 was sparged with N_2 for 30 min. The mixture was added to the 2-neck flask using a cannula, and the reaction was refluxed at 95°C and stirred for 3 h. The reaction was then opened to air and the dioxane was removed via rotary evaporation. Ethyl acetate (100 mL) was added to the flask and the mixture was filtered to remove the precipitated solid. The reaction mixture was transferred to a separatory funnel and the organic phase was separated from the aqueous phase. The aqueous phase was extracted with ethyl acetate (2 x 100 mL), and the combined organic extracts were then dried over $MgSO_4$ and concentrated *in vacuo*. The residue was purified by silica gel flash column chromatography, eluting with a 5-10% ethyl acetate in hexanes gradient. **6** was obtained as a white crystalline solid. (Yield: 1.92 g, 57%)

^{1}H NMR (400 MHz, $CDCl_3$): δ (ppm) 7.55 (d, J = 8.5 Hz, 2H), 7.48 (d, J = 8.4 Hz, 2H), 7.43 (d, J = 8.5 Hz, 2H), 7.32 (d, J = 8.4 Hz, 2H), 2.52 (s, 3H). ^{13}C{^{1}H} NMR (101 MHz, $CDCl_3$): δ (ppm) 139.46, 138.24, 136.74, 131.91, 128.39, 127.24, 126.98, 121.41, 15.84.

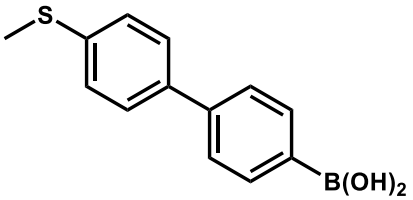

7

7. Synthesized following the same procedure as **3**, starting from **6** (1.0 g, 3.58 mmol). **7** was obtained as a white fluffy powder. (Yield: 664 mg, 76%)

^{1}H NMR (400 MHz, DMSO-d_6): δ (ppm) 8.03 (s, 2H), 7.86 (d, J = 7.7 Hz, 2H), 7.63 (dd, J = 10.5, 8.0 Hz, 4H), 7.35 (d, J = 8.5 Hz, 2H), 2.51 (s, 3H). ^{13}C{^{1}H} NMR (101 MHz, DMSO-d_6): δ (ppm) 140.83, 137.61, 136.53, 134.74, 132.97 127.05, 126.35, 125.20, 14.64.

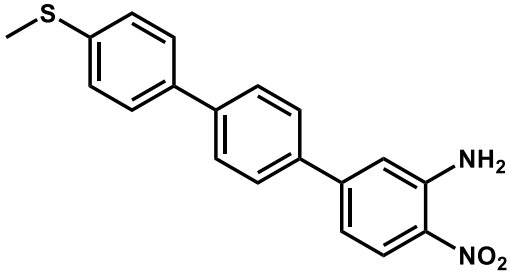

8

8. Synthesized following the same procedure as **4**, starting from **7** (265 mg, 2.0 mmol) and 5-chloro-2-nitroaniline (448mg, 2.6 mmol) with the following modifications. The solvent mixture used for the reaction is: 40 mL of dioxane, 100 μL of benzene and 10 mL of a 2.0 M aqueous K_2CO_3. After stirring under reflux for 18 h, the reaction mixture was hot filtered and dioxane was removed by rotary evaporation. The precipitated solid was collected by filtration, washed with water (3 x 50 mL), and diethyl ether (3 x 50 mL). The solid was then redissolved in 150 mL of DCM, dried over $MgSO_4$, filtered, and the solvent was removed by rotary evaporator. The resulting solid was dried *in vacuo*. **8** was obtained as a bright yellow crystalline solid. (Yield: 405 mg, 78%)

^{1}H NMR (500 MHz, DMSO-d_6): δ (ppm) 8.06 (d, J = 9.0 Hz, 1H), 7.81 (d, J = 8.5 Hz, 2H), 7.74 (d, J = 8.2 Hz, 2H), 7.72–7.68 (m, 3H), 7.49 (s, 2H), 7.40–7.33 (m, 3H), 6.99 (dd, J = 9.0, 2.0 Hz, 1H), 2.52 (s, J = 1.2 Hz, 3H). ^{13}C{^{1}H} NMR (126 MHz, DMSO-d_6): δ (ppm) 146.47, 146.32, 139.90, 138.11, 136.94, 135.59, 129.53, 127.39, 127.06, 126.92, 126.35, 126.30, 116.16, 114.30, 14.60.

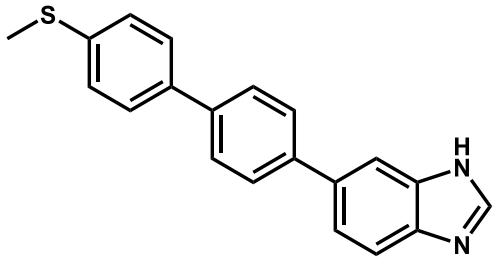

9

9. Synthesized following the same procedure as **5**, starting from **8** (250 mg, 790 μmol) with the following modifications. Benzene (100 μL) was added to the reaction to aid solubilizing the amine. After refluxing for 12 h, the mixture was hot filtered. The solid product was washed with ethyl acetate to remove excess starting material. **9** was obtained as a light yellow-orange powder. (Yield: 205 mg, 88%)

^{1}H NMR (500 MHz, DMSO-d_6): δ (ppm) 8.26 (s, 1H), 7.97 (br, 1H), 7.77 (dd, J = 9.6, 8.5 Hz, 4H), 7.69 (d, J = 8.2 Hz, 3H), 7.64–7.56 (m, 1H), 7.37 (d, J = 8.1 Hz, 2H), 2.52 (s, 3H). ^{13}C{^{1}H} NMR (101 MHz, DMSO-d_6): δ (ppm) 143.29, 137.92, 137.37, 136.64, 136.40, 130.72, 127.87, 127.02, 126.92, 126.88, 126.85, 121.99, 121.06, 119.82, 112.46, 15.37.

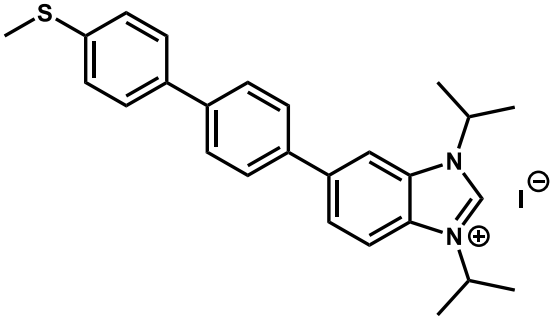

NHC2-HI

NHC2–HI. Synthesized following the same procedure as **NHC0–HI**, starting from **9** (100 mg, 316 μmol) with the following modifications. The reaction was stirred under reflux until consumption of the starting benzimidazole, as determined by NMR (typically ~72 h). An additional 4 equivalents of 2-iodopropane were added after 48 h. The product was precipitated using ethyl acetate. **NHC2–HI** was obtained as a white powder. (Yield: 24 mg, 14%)

^{1}H NMR (500 MHz, $CDCl_3$): δ (ppm) 11.10 (s, 1H), 7.92 (d, J = 8.7 Hz, 2H), 7.87 (d, J = 8.9 Hz, 1H), 7.76 (d, J = 7.8 Hz, 2H), 7.71 (d, J = 7.9 Hz, 2H), 7.61 (d, J = 8.2 Hz, 2H), 7.40 (d, J = 8.7 Hz, 2H), 5.27 (overlapping septets, 2H), 2.57 (s, 3H), 1.95 (overlapping doublets, 12H). ^{13}C{^{1}H} NMR (126 MHz, $CDCl_3$): δ (ppm) 140.85, 140.42, 140.37, 137.86, 136.69, 133.20, 131.65, 130.33, 128.03, 127.66, 127.39, 126.94, 126.75, 114.18, 111.72, 52.79, 52.55, 22.39, 22.39, 15.77.

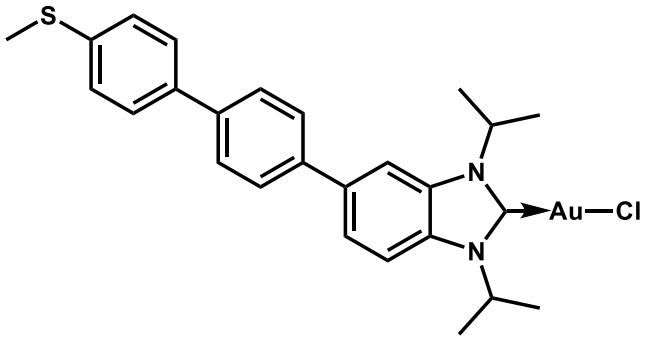

NHC2-AuCl

NHC2–AuCl. NHC2–AuCl was prepared following the general procedure outlined above for the synthesis of **NHC1–AuCl**, starting from **NHC2–HI** (10 mg, 18 μmol) KtOBu (2 mg, 21 μmol), and (SMe_2)AuCl (6 mg, 20 μmol). **NHC2–AuCl** was obtained as a white powder. (Yield: 11 mg, 90%)

X-ray diffraction quality crystals were grown by slow evaporation of a DCM solution of **NHC2–AuCl**.

^{1}H NMR (500 MHz, $CDCl_3$): δ (ppm) 7.84 (s, 1H), 7.73 (m, 3H), 7.68 (d, J = 7.7 Hz, 2H), 7.65 (d, J = 8.8 Hz, 1H), 7.61 (d, 2H), 7.39 (d, J = 7.9 Hz, 2H), 5.57 (overlapping septets, 2H), 2.57 (s, 3H), 1.81 (overlapping doublets, 12H). ^{13}C{^{1}H} NMR (126 MHz, $CDCl_3$): δ (ppm) 176.82, 140.17, 139.09, 138.23, 137.46, 137.01, 132.52, 131.73, 127.92, 127.47, 127.35, 126.95, 123.50, 113.30, 111.28, 54.58, 54.34, 21.81, 21.73, 15.82.

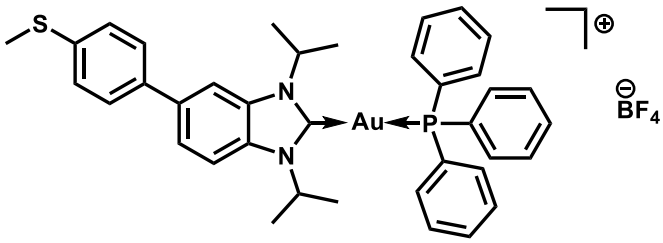

[NHC1-AuPPh$_3$][BF$_4$]

[NHC1–AuPPh$_3$][BF$_4$]. Synthesized following a modified literature procedure.[5] **NHC1–AuCl** (20 mg, 35 μmol) was dissolved in 5 mL of THF. In a separate vial, PPh_3 (9 mg, 36 μmol) and $AgBF_4$ (7 mg, 35 μmol) were dissolved in 5 mL of THF. This solution was added dropwise to the **NHC1–AuCl** solution and the reaction was stirred for 1 h, protected from light. The solution was then filtered, and the solvent was removed *in vacuo*. The residue was washed with hexanes. The resulting solid (yield: 22 mg, 73%) was a mixture of **[NHC1–AuPPh$_3$][BF$_4$]**, **[(NHC1)$_2$–Au][BF$_4$]**, and **[(PPh$_3$)$_2$Au][BF$_4$]**, as determined by NMR spectroscopy and reported

characterization.[6] The **[NHC1–AuPPh$_3$][BF$_4$]**:**[(NHC1)$_2$–Au][BF$_4$]**:**[(PPh$_3$)$_2$Au][BF$_4$]** ratio in the final product is ca. 3:1:1. This mixture was used without further purification for the STM-BJ control experiment as **[NHC1–AuPPh$_3$][BF$_4$]** and **[(NHC1)$_2$–Au][BF$_4$]** should have the same conductance and **[(PPh$_3$)$_2$Au][BF$_4$]** will not conduct.

^{1}H NMR (400 MHz, $CDCl_3$): δ (ppm) 7.85–7.77 (m, 2H), 7.68–7.41 (bm, 15H), 7.67 (m, 1H), 7.56 (d, *J* = 8.4 Hz, 2H), 7.38 (d, *J* = 8.3 Hz, 2H), 5.34 (m, 2H), 2.54 (s, 3H), 1.94–1.83 (m, 12H). ^{13}C{^{1}H} NMR (101 MHz, $CDCl_3$): δ (ppm) 187.57, 138.78, 138.54, 136.62, 134.03, 133.29, 132.61, 131.73, 129.86, 127.89, 127.06, 124.77, 113.49, 110.75, 53.42, 53.24, 23.31, 23.16, 15.79. ^{31}P{^{1}H} NMR (162 MHz, $CDCl_3$): δ (ppm) 40.09.

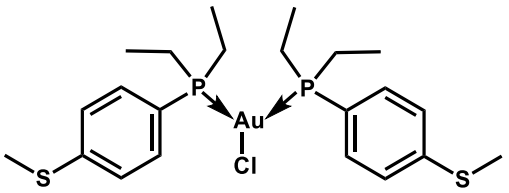

((4-MeSPh)Et$_2$P)$_2$AuCl

((4-MeSPh)Et$_2$P)$_2$AuCl. Prepared by adding a solution of diethyl(4-(methylthio)phenyl)phosphine[7] (79 mg, 370 μmol) in THF to a suspension of $(SMe)_2AuCl$ (100 mg, 340 μmol) in THF. The reaction was stirred for 2 h. The suspension was then filtered and the solvent was removed *in vacuo*. The oily residue was dissolved in THF (~1 mL), layered with diethyl ether and placed in a freezer (-35°C) to crystallize. **((4-MeSPh)Et$_2$P)$_2$AuCl** was obtained as colorless crystals that melt at room temperature. (Yield: 33 mg, 13%)

^{1}H NMR (500 MHz, C_6D_6): δ (ppm) 7.51 (dd, *J* = 11.2, 8.1 Hz, 2H), 6.99 (d, *J* = 6.7 Hz, 2H), 1.90 (s, 3H), 1.87–1.56 (dm, 4H), 0.89 (dt, *J* = 19.6, 7.5 Hz, 6H). ^{13}C{^{1}H} NMR (126 MHz, C_6D_6): δ (ppm) 133.64, 133.54, 125.63, 125.54, 20.76, 20.49, 14.01, 8.96. ^{31}P{^{1}H} NMR (202 MHz, C_6D_6): δ (ppm) 38.10.

2. Instrumentation

^{1}H, ^{13}C, and ^{31}P NMR spectra were recorded on Bruker DRX400 and DMX500 spectrometers. ^{1}H and ^{13}C spectra were referenced using DMSO-d_6, C_6D_6, or $CDCl_3$, with the residual solvent peak as the internal standard, and ^{31}P spectra were referenced using H_3PO_4. Chemical shifts were reported in ppm, with ^{1}H multiplicities reported as: s (singlet), d (doublet), t (triplet), q (quartet),

p (pentet), m (multiplet), and br (broad) or as indicated. Coupling constants, *J*, are reported in Hz and integration is provided.

3. Single Crystal X-Ray Diffraction

Single crystal x-ray diffraction data was collected on an Agilent SuperNova diffractometer using mirror-monochromated CuK_α or MoK_α radiation. Data collection, integration, scaling (ABSPACK) and absorption correction (face-indexed Gaussian integration[8] or numeric analytical methods[9]) were performed in CrysAlisPro.[10] Structure solution was performed using ShelXT.[11] Subsequent refinement was performed by full-matrix least-squares on F^2 in ShelXL.[11] Olex2[12] was used for viewing and to prepare CIF files. Many disordered molecules were modeled as rigid fragments from the Idealized Molecular Geometry Library.[13] ORTEP graphics were prepared in CrystalMaker.[14] Thermal ellipsoids are rendered at the 50% probability level. Details of crystallographic data and parameters for data collection and refinement are provided in Table S1.

Crystals were mounted on MiTeGen mounts with the aid of STP oil and cooled to 100 K on the diffractometer for screening and data collection, except in the case of **NHC1–AgCl** which was collected at room temperature. A minimum of 1 hemisphere of data to 0.8 Å resolution was collected for all compounds.

Structure solution and space group assignment were typically performed in ShelXT with no difficulty. In the final refinements, non-H atoms were refined anisotropically with no restraints unless noted; C-H hydrogens were placed in calculated positions and refined with riding isotropic ADPs and coordinates. The non-routine details of the refinements are given below:

NHC1–AuCl. Extinction correction was refined to 0.0090(8).

NHC2–AuCl. A molecule of dichloromethane was located in difference maps and modeled in two disordered positions. Each independent position was modeled as a rigid fragment with coordinates taken from the Idealized Molecular Geometry Library.
The final refinement had significant Fourier difference features (+/- 3-4 e- A-3) within 1-2 A of the gold atom. We could not identify any common reason (twinning, absorption) for these features

and we conclude that the structure may suffer a whole-molecule disorder with an occupancy around 5% or less for the minor component. We were unable to build a disordered model that accounted for these difference features. However, the atomic positions and ADPs of the major component appear well-behaved in spite of the strongly featured difference map.

NHC1–CuCl. The terminal $C_6H_4SCH_3$ moiety was disordered over two positions in a 3:1 ratio. These were modeled with the following restraints: the two independent positions were made equivalent with SAME instructions; the anisotropic ADPs of the major component were stabilized with RIGU; the minor component was modeled with isotropic ADPs which were stabilized with SIMU. Each 8-atom C-C_6H_4-S group was also stabilized with a FLAT instruction.

((4-MeSPh)Et$_2$P)$_2$AuCl. The asymmetric unit contains two independent ((4-MeSPh)Et$_2$P)$_2$AuCl molecules and four molecules of THF. One of the THFs is disordered over two positions in a near 1:1 ratio; these were modeled with the aid of SAME and RIGU restraints and a short-range SIMU instruction for overlapping ADPs.

Table S1. Selected Crystallographic Data

Compound	NHC0–AuCl	NHC1–AuCl	NHC2–AuCl
Formula	$C_{14}H_{20}AuClN_2S$	$C_{20}H_{24}N_2SClAu$	$C_{27}H_{30}AuCl_3N_2S$
MW	480.8	556.89	717.9
Space group	P-1	P-1	C2/c
***a* (Å)**	9.3400(5)	8.5453(3)	32.2745(12)
***b* (Å)**	9.4284(5)	10.0951(3)	7.7536(2)
***c* (Å)**	9.9843(5)	12.3151(4)	23.0815(7)
***α* (°)**	80.472(4)	104.024(3)	90
***β* (°)**	72.891(5)	106.985(3)	109.981(4)
***γ* (°)**	73.520(4)	94.210(3)	90
V (Å^3)	802.56(8)	973.77(6)	5428.4(3)
Z	2	2	8
ρ_{calc} (g cm^{-3})	1.99	1.899	1.757
T (K)	100	100.0(2)	99.9(2)
λ (Å)	1.54184	1.54184	1.54184
$2\theta_{min}$, $2\theta_{max}$	9.306, 146.01	7.81, 145.894	8.152,146.286
Nref	6986	8851	36522
R(int), R(σ)	0.0335, 0.0391	0.0277, 0.0273	0.0383, 0.0258
μ(mm^{-1})	19.868	16.486	13.762
Size (mm)	0.16 × 0.128 × 0.078	0.369 × 0.16 × 0.093	0.162 × 0.081 × 0.015
T_{max}, T_{min}	0.758, 0.355	0.638, 0.100	0.810, 0.275
Data	3175	3877	5405
Restraints	0	0	32
Parameters	177	232	334
R_1(obs)	0.0406	0.0239	0.0586
wR_2(all)	0.1055	0.0616	0.1522
S	1.064	1.115	1.118
Peak, hole (e$^-$ Å^{-3})	1.95, -3.58	0.9, -1.09	3.35, -3.71
CCDC deposition #	1832127	1832128	1832129

Compound	NHC1–CuCl	NHC1–AgCl	((4-SMePh)Et$_2$P)$_2$AuCl
Formula	$C_{20.5}H_{25}Cl_2CuN_2S$	$C_{21}H_{26}AgCl_3N_2S$	$C_{30}H_{50}AuClO_2P_2S_2$
MW	465.92	1105.43	801.17
Space group	$P2_1/c$	$P2_1/n$	$P2_1/c$
***a* (Å)**	12.3475(8)	14.2598(6)	22.3899(2)
***b* (Å)**	7.5762(7)	11.7679(5)	17.95980(10)
***c* (Å)**	23.0412(16)	15.0014(7)	18.6379(2)
***α* (°)**	90	90	90
***β* (°)**	104.263(7)	106.365(5)	111.6290(10)
***γ* (°)**	90	90	90
V (Å^3)	2089.0(3)	2415.37(19)	6966.94(11)
Z	4	4	8
ρ_{calc} (g cm^{-3})	1.481	1.52	1.528
T (K)	100.0(2)	293.94(19)	99.97(10)
λ (Å)	0.71073	1.54184	1.54184
$2\theta_{min}$, $2\theta_{max}$	6.81, 59.308	6.636, 59.204	7.09, 145.846
Nref	9914	11063	94068
R(int), R(σ)	0.0665, 0.1169	0.0283, 0.0468	0.0542, 0.0331
μ(mm^{-1})	1.409	1.262	10.814
Size (mm)	0.251 × 0.071 × 0.027	0.384 × 0.175 × 0.088	0.256 × 0.131 × 0.092
T_{max}, T_{min}	1.0, 0.805	0.979, 0.954	0.452, 0.183
Data	4913	5599	13776
Restraints	156	0	156
Parameters	284	259	743
R_1(obs)	0.068	0.0533	0.0363
wR_2(all)	0.1621	0.144	0.0942
S	1.062	1.085	1.103
Peak, hole (e$^-$ Å^{-3})	0.93, -1.13	0.83, -0.64	2.79, -1.23
CCDC deposition #	1832131	1832132	1832130

Crystal Structures: All thermal ellipsoids are rendered at the 50% probability level.

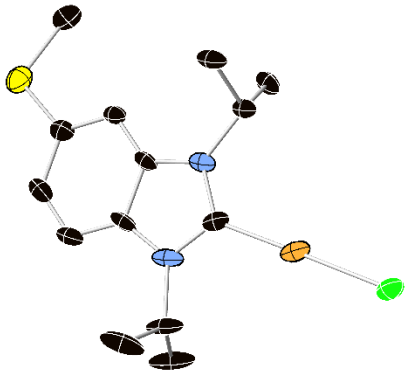

Figure S2: Crystal structure of NHC0–AuCl. Colour code: Au, gold; Cl, green; S, yellow; N, light blue; C, black. H atoms are removed for clarity.

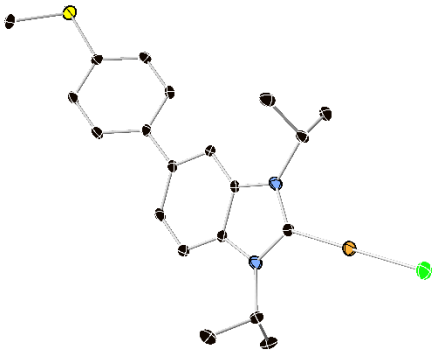

Figure S3: Crystal structure of NHC1–AuCl. Colour code: Au, gold; Cl, green; S, yellow; N, light blue; C, black. H atoms are removed for clarity.

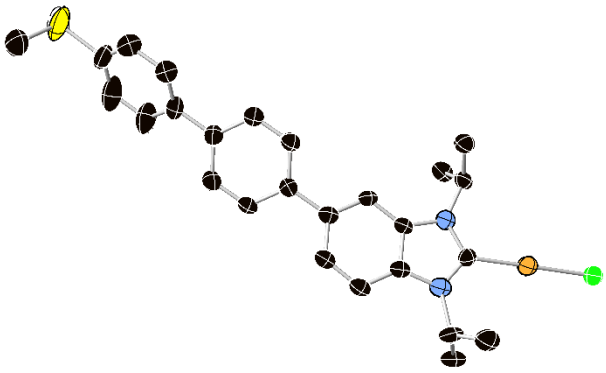

Figure S4: Crystal structure of NHC2–AuCl. Colour code: Au, gold; Cl, green; S, yellow; N, light blue; C, black. H atoms are removed for clarity.

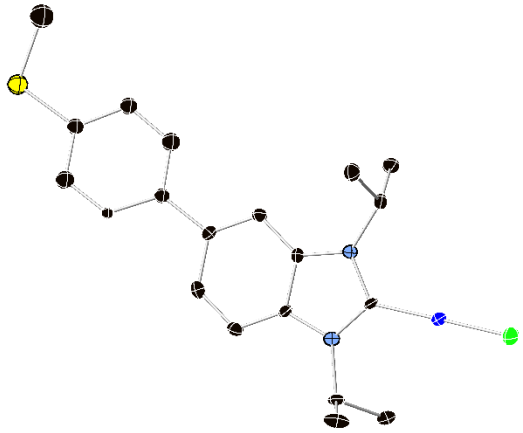

Figure S5: Crystal structure of NHC1–CuCl. Colour code: Cu, dark blue; Cl, green; S, yellow; N, light blue; C, black. H atoms are removed for clarity.

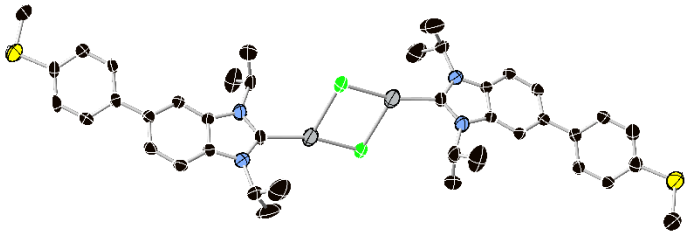

Figure S6: Complete crystal structure of NHC1–AgCl. Colour code: Ag, grey; Cl, green; S, yellow; N, light blue; C, black. H atoms are removed for clarity.

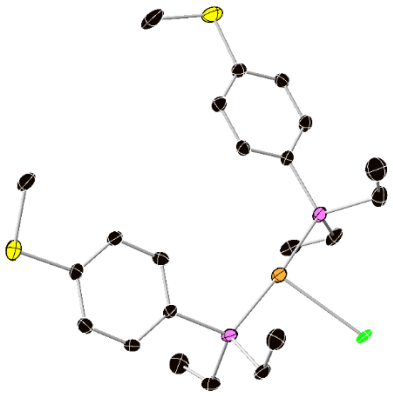

Figure S7: Crystal structure of $((4\text{-MeSPh})Et_2P)_2AuCl$. Colour code: Au, gold; Cl, green; S, yellow; P, pink; C, black. H atoms are removed for clarity.

4. Additional STM-BJ Data

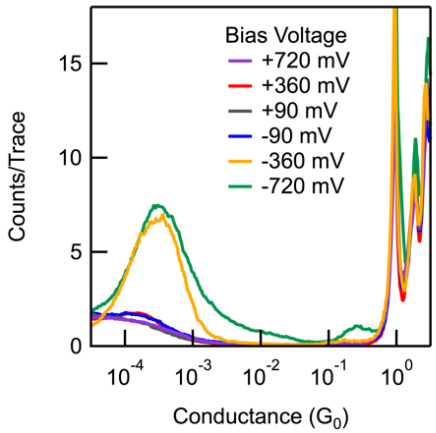

Figure S8: Bias Dependence. Conductance histograms for **NHC1–AuCl** as a function of tip bias measured in PC.

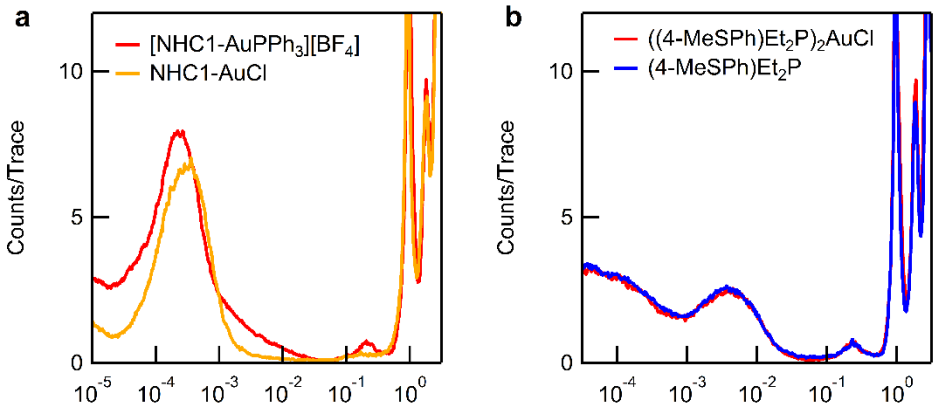

Figure S9: Control Measurements. **(a)** Conductance histogram for [**NHC1–AuPPh$_3$][BF$_4$]** compared with that of **NHC1–AuCl** measured in PC at –360 mV tip bias. **(b)** Conductance histograms of the complex **((4-MeSPh)Et$_2$P)$_2$AuCl** and the free ligand **(4-MeSPh)Et$_2$P** (without a AuCl terminal group) measured in PC at –360 mV tip bias.

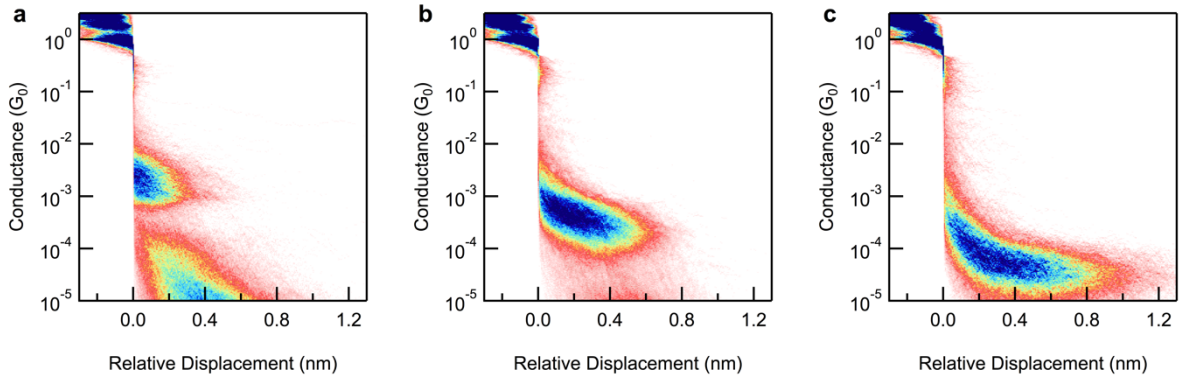

Figure S10: Conductance-displacement of NHC*n*–AuCl. Two-dimensional conductance-displacement histograms for **(a) NHC0–AuCl**, **(b) NHC1–AuCl** and **(c) NHC2–AuCl**. Corresponding 1D histograms are shown in Figure 3b.

5. Additional Computational Data

Calculation of junction binding energies: In order to determine the individual contributions of NHC and SMe terminations to the binding energy, three different junction terminations were considered: (a) A molecule terminated with two NHC linkers, (b) a molecule terminated with two

SMe linkers, or (c) molecules with one NHC and one SMe linker. Exemplary junction structures are shown in Figure S11.

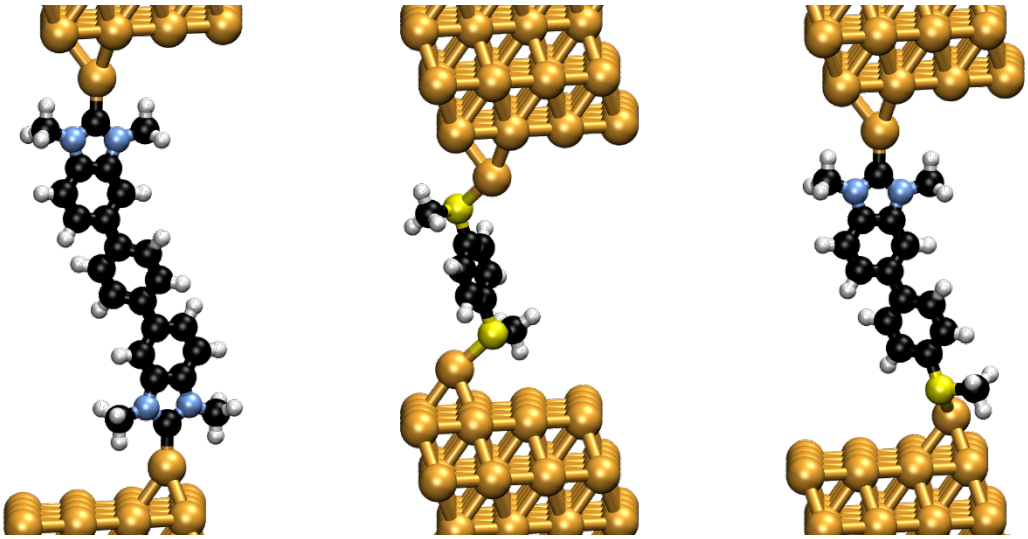

Figure S11: Junction structures used to calculate molecular binding energies. (a) A biscarbene junction with one phenyl group. (b) A bis-SMe junction with one phenyl group. (c) An **NHC1–Au** junction.

Values of the binding energy of these junctions with different numbers of phenyl groups are given in Table S2 and include corrections to basis set superposition errors.[15] Positive values denote stable junctions with respect to the Au structure and isolated molecules. From the junctions with equal linker groups at both ends, the binding energy of a single NHC or SMe bond to Au is evaluated. For the junctions realized in experiment, most of the binding energy comes from the NHC-Au bond.

Table S2: Calculated binding energies (eV).

Number of Phenyls	NHC-NHC	SMe-SMe	NHC-SMe
0	4.19		2.88
1	4.14	1.43	2.73
2	4.17	1.40	2.69
Average	4.17	1.42	2.77
Average per bond	2.08	0.71	

The binding energies of the **NHC1–Au**, **NHC1–Ag** and **NHC1–Cu** junctions are 2.73, 2.35 and 2.75 eV, respectively. Subtracting the contribution of the SMe-Au contact, the binding energies of the NHC–Au, NHC–Ag and NHC–Cu bonds are 2.02, 1.64 and 2.04 eV. These results follow the trend in bond strength of M = Cu ≈ Au > Ag measured and calculated previously for nitrene fragments to a IMesM+ moiety.[16]

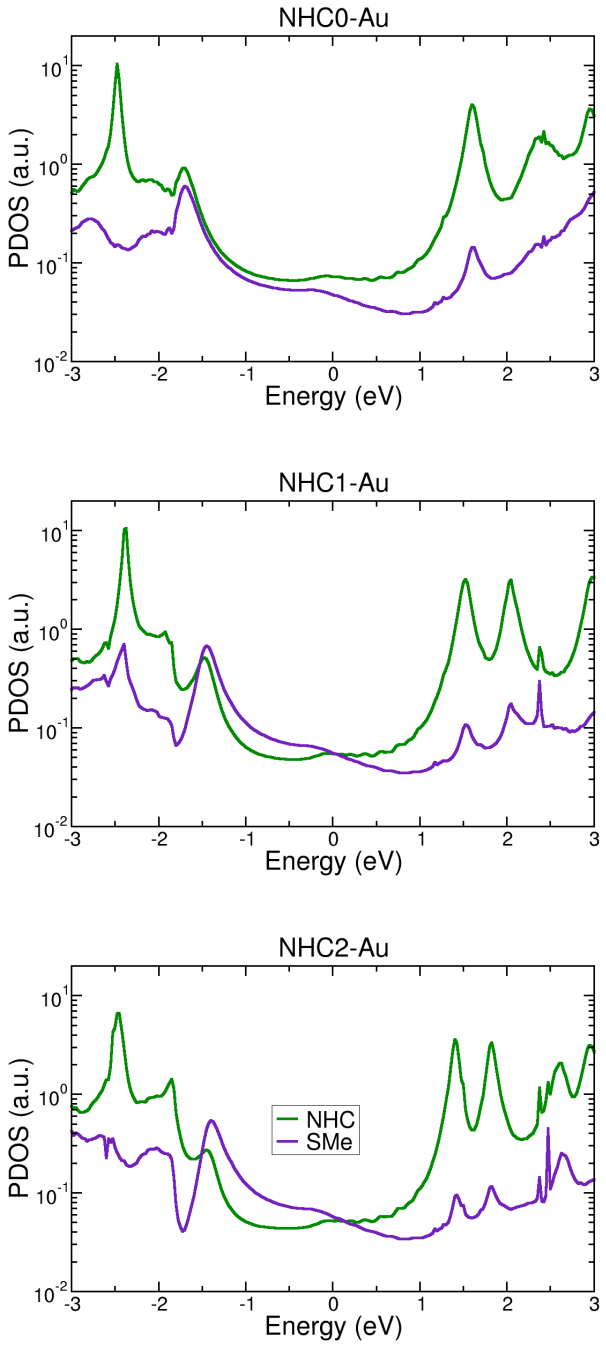

Figure S12: Projected density of states (PDOS) onto NHC and SMe linkers. PDOS onto the molecular atoms forming the NHC and on the SMe terminations, calculated from the Green's function. NHC features dominate the spectrum near the gap, except near –1.5 eV, where SMe states are important, more so for longer molecules.

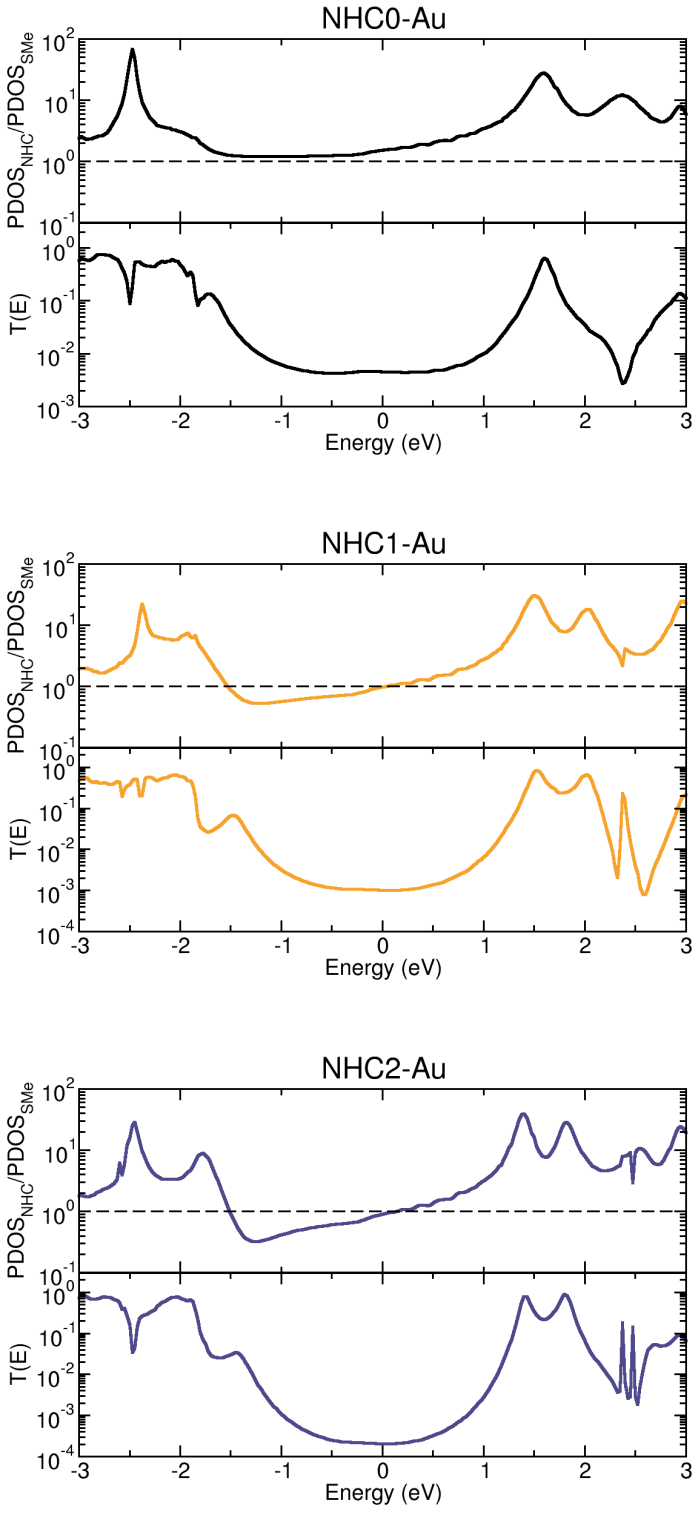

Figure S13: Ratio of NHC and SMe PDOS. Ratio of the PDOS on the NHC to the SMe units (top panels) and calculated transmission spectra (bottom panels).

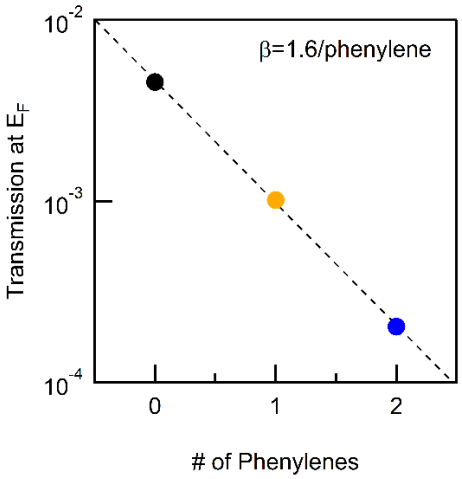

Figure S14: Exponential fit to calculated transmission values at E_f.

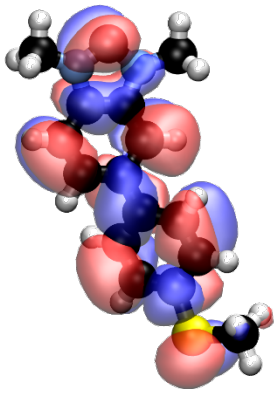

Figure S15: LUMO of the NHC1 free carbene.

Calculation of projected transmission functions.

We calculate the electronic transmission through molecular orbitals by projecting the electronic coupling matrix to the electrode for the NHC- or SMe-terminated contacts ($\Gamma_{NHC,SMe}$) onto eigenstates of the **NHC1** molecule. In the expression for the transmission function, one can introduce the completeness relation to obtain

$$T = tr[G\Gamma_{NHC}G^{\dagger}\Gamma_{SMe}] = tr\left[G\sum_i|\psi_i\rangle\langle\psi_i|\Gamma_{NHC}\sum_j|\psi_j\rangle\langle\psi_j|G^{\dagger}\sum_k|\psi_k\rangle\langle\psi_k|\Gamma_{SMe}\sum_l|\psi_l\rangle\langle\psi_l|\right]$$

where ψ_i form a complete and orthogonal basis in a subspace of the full device (such as the molecule). For clarity, the dependence on energy and k-points is omitted. The matrix elements $\langle\psi_i|\Gamma_{NHC,SMe}|\psi_j\rangle$ represent the electronic coupling of eigenstates *i* and *j* to the leads on the NHC- or SMe-terminated contacts. Transmission through specific molecular orbitals is given by diagonal

terms $\langle\psi_i|\Gamma_{NHC,SMe}|\psi_i\rangle$. Because these projections include only some terms of the total transmission, at certain energies the projected transmission can be higher than the total, indicating that other terms which decrease transmission are included in the projection.[17,18]

Figure S16 shows the calculated spectra projecting the coupling matrix of either the NHC- or SMe-terminated contacts, onto the **NHC1** HOMO. From the spectral analysis, the HOMO is localized mostly on the SMe linker. The transmission spectra projected onto the HOMO are much smaller than the total transmission, even at energies close to the HOMO resonance around –1.5 eV, demonstrating that this orbital is not well coupled to either electrode.

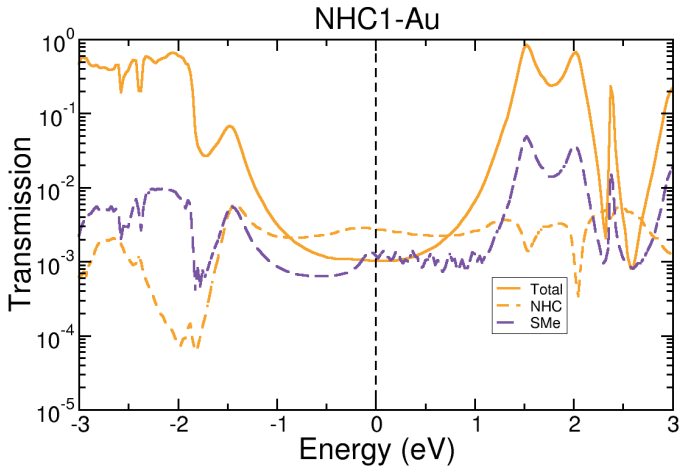

Figure S16: Calculated transmission spectra of **NHC1–Au** projecting the coupling matrices Γ at the NHC- or SMe-terminated contacts onto the HOMO of **NHC1**.

Figure S17 shows the calculated spectra projecting the coupling matrices onto the **NHC1** LUMO. Remarkably, the LUMO alone provides almost the total electronic transparency of the junction over more than 1 eV. This demonstrates that the NHC termination, which sets the character of the LUMO, provides excellent coupling for electron transport.

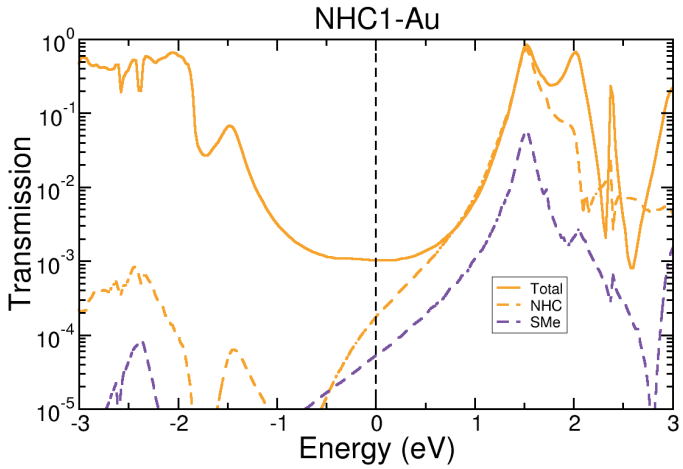

Figure S17: Calculated transmission spectra of **NHC1–Au** projecting the coupling matrices Γ at the NHC- or SMe-terminated contacts onto the LUMO of **NHC1**.

6. References

(1) Chakraborty, P. Sodium Methanethiolate. In *Encyclopedia of Reagents for Organic Synthesis*; John Wiley & Sons, Ltd: Hoboken, 2001; doi:10.1002/047084289X.rn01716.

(2) Crudden, C. M.; Horton, J. H.; Ebralidze, II; Zenkina, O. V.; McLean, A. B.; Drevniok, B.; She, Z.; Kraatz, H. B.; Mosey, N. J.; Seki, T.; Keske, E. C.; Leake, J. D.; Rousina-Webb, A.; Wu, G. Ultra stable self-assembled monolayers of N-heterocyclic carbenes on gold. *Nature Chem.* **2014**, 6, 409-414.

(3) Kuntz, K.; Emmitte, K. A.; Rheault, T. R.; Smith, S.; Hornberger, K.; Dickson, H.; Cheung, M. Benzimidazole thiophene compounds. U.S. Patent 2008300247, December 4, 2004.

(4) Gonell, S.; Poyatos, M.; Peris, E. Triphenylene-based tris(N-heterocyclic carbene) ligand: unexpected catalytic benefits. *Angew. Chem. Int. Ed.* **2013**, 52, 7009-7013.

(5) Jahnke, M. C.; Pape, T.; Hahn, F. E. Ligand exchange at a gold(I) carbene complex. *Z Naturforsch., B: Chem. Sci.* **2013**, 68, 467-473.

(6) Gaillard, S.; Nun, P.; Slawin, A. M. Z.; Nolan, S. P. Expeditious synthesis of $[Au(NHC)(L)]^+$ (NHC = N-heterocyclic carbene; L = phosphine or NHC) complexes. *Organometallics* **2010**, 29, 5402-5408.

(7) Roy, X.; Schenck, C. L.; Ahn, S.; Lalancette, R. A.; Venkataraman, L.; Nuckolls, C.; Steigerwald, M. L. Quantum soldering of individual quantum dots. *Angew. Chem. Int. Ed.* **2012**, 51, 12473-12476.

(8) Blanc, E.; Schwarzenbach, D.; Flack, H. D. The evaluation of transmission factors and their first derivatives with respect to crystal shape parameters. *J. Appl. Crystallogr.* **1991**, 24, 1035-1041.

(9) Clark, R. C.; Reid, J. S. The analytical calculation of absorption in multifaceted crystals. *Acta. Crystallogr., Sect. A: Found. Crystallogr.* **1995**, 51, 887-897.

(10) *CrysAlisPro*, version 1.171.37.35; Oxford Diffraction /Agilent Technologies UK Ltd.: Yarnton, England, 2014.

(11) Sheldrick, G. SHELXT - Integrated space-group and crystal-structure determination. *Acta. Crystallogr., Sect. A: Found. Crystallogr.* **2015**, 71, 3-8.
(12) Dolomanov, O. V.; Bourhis, L. J.; Gildea, R. J.; Howard, J. A. K.; Puschmann, H.; OLEX2: a complete structure solution, refinement and analysis program. *J. Appl. Crystallogr.* **2009**, 42, 339-341.
(13) Guzei, I. An idealized molecular geometry library for refinement of poorly behaved molecular fragments with constraints. *J. Appl. Crystallogr.* **2014**, 47, 806-809.
(14) *CrystalMaker*, version 9.2.5 (653); CrystalMaker Software Ltd.: Oxford, England, 2015.
(15) van Duijneveldt, F. B.; van Duijneveldt-van de Rijdt, J. G. C. M.; van Lenthe, J. H. State of the art in counterpoise theory. *Chem Rev* **1994**, 94, 1873-1885.
(16) Fedorov, A.; Couzijn, E. P. A.; Nagornova, N. S.; Boyarkin, O. V.; Rizzo, T. R.; Chen, P. Structure and bonding of isoleptic coinage metal (Cu, Ag, Au) dimethylaminonitrenes in the gas phase. *J. Am. Chem. Soc* **2010**, 132, 13789-13798.
(17) Schneider, N. L.; Neel, N.; Andersen, N. P.; Lu, J. T.; Brandbyge, M.; Kroger, J.; Berndt, R. Spectroscopy of transmission resonances through a C-60 junction. *J. Phys.: Condens. Matter* **2015**, 27, 015001.
(18) Papior, N., Lorente, N., Frederiksen, T., Garcia, A. & Brandbyge, M. Improvements on non-equilibrium and transport Green function techniques: The next-generation TRANSIESTA. *Comput. Phys. Commun.* **2017**, 212, 8-24.